

A Model for Dwarf Spheroidal Satellite Galaxies Without Dark Matter

Ralf S. Klessen

Max-Planck-Institut für Astronomie, Königstuhl 17, D-69117 Heidelberg, Germany

e-mail: klessen@mpia-hd.mpg.de

Abstract

Self-consistent simulations of the dynamical evolution of low-mass satellite galaxies without dark matter on different orbits interacting with an extended Galactic dark halo are described. The calculations proceed for many orbital periods until well after the satellite dissolves. In all cases the dynamical evolution converges to a remnant that contains roughly 1 per cent of the initial satellite mass. The stable remnant results from severe tidal shaping of the initial satellite. To an observer from Earth these remnants look strikingly similar to the Galactic dwarf spheroidal satellite galaxies. Their apparent mass-to-light ratios are very large despite the fact that they contain no dark matter.

These computations show that a remnant without dark matter displays larger line-of-sight velocity dispersions σ for more eccentric orbits, which is a result of projection onto the observational plane. Assuming they are not dark matter dominated, it follows that the Galactic dSph satellites with $\sigma > 6$ km/s should have orbital eccentricities of $e > 0.5$. Some remnants have sub-structure along the line-of-sight that may be apparent in the morphology of the horizontal branch.

1 Introduction

At least about ten dwarf spheroidal (dSph) galaxies are known to orbit the Milky Way at distances ranging from a few tens to a few hundred kpc. On the sky they are barely discernible stellar density enhancements. Some have internal substructure and appear flattened. Their velocity dispersions and stellar masses are similar to those seen in globular clusters. However, they are about two orders of magnitude more extended. For spherical systems in virial equilibrium with an isotropic velocity dispersion, the overall mass of the system can be determined from the observed velocity dispersion. Comparing this ‘gravitational’ mass to the luminosity of the system determines the mass-to-light ratio M/L , which for the solar neighborhood is $3 < M/L < 5$ (e.g. Tsujimoto et al. 1997). For the dSph satellites, M/L values as large as a few hundred are inferred, leading to the conclusion that these systems may be completely dark matter dominated (see Da Costa 1998, Ferguson & Binggeli 1994, Grebel 1997, Irwin & Hatzidimitriou 1995, Mateo 1998a,b, Pryor 1994).

An alternative might be that the assumption of virial equilibrium is violated for the Galactic satellite galaxies: they could be significantly perturbed by Galactic tides. Indeed, departures of the dSph stellar density profiles from the best-fitting King models are commonly interpreted as existence of ‘extra-tidal’ stars implying that most dSph galaxies could be significantly losing mass (Irwin & Hatzidimitriou 1995, Kuhn et al. 1996, Smith et al. 1997, Burkert 1997). However, this is still under debate (Olszewski 1998, Pryor private communication).

The ‘tidal scenario’ has been studied in detail by a variety of authors: Oh et al. (1995) modeled the evolution of dSph galaxies on different orbits in a set of rigid spherical Galactic potentials, using 10^3 particles for the satellites. Piatek & Pryor (1995) concentrate on one

perigalactic passage of a dSph galaxy in different Galactic potentials. Their satellite consists of 10^4 particles. They find that a single perigalactic passage cannot perturb a satellite significantly enough for an observer to measure a high M/L ratio, reaching similar conclusions as Oh et al. (1995). Johnston et al. (1995) and Johnston (1997) are studying the overall distribution of tidal debris from disrupted dwarf galaxies in a Galactic halo.

2 A Scenario for dSph Galaxies as Remnants of Dissolved Satellites

High-resolution simulations of the long-term evolution of a low-mass satellite galaxy on different orbits interacting with an extended Galactic dark halo are presented by Kroupa (1997; hereafter K97) and by Klessen & Kroupa (1998; hereafter KK98). The satellites are modeled by 1.3×10^5 up to 2.0×10^6 particles and the orbital eccentricities are in the range $0.41 \leq e \leq 0.96$. The simulations were performed using a particle-mesh code with nested sub-grids and a direct-summation N -body code running with the special purpose hardware device GRAPE (Sugimoto et al. 1990, Ebisuzaki et al. 1993). Initially, the satellite is spherical with an isotropic velocity distribution. It has a mass of $10^7 M_\odot$ and a *true* mass-to-light ratio of $(M/L)_{\text{true}} = 3.0$. The calculations proceed for many orbital periods until well after the satellite became unbound. The aim is to study the system well after the satellite has mostly dissolved and to ‘observe’ its properties as it would be seen from Earth. The satellite is projected onto the sky and its brightness profile, line-of-sight velocity dispersion and *apparent* M/L ratio are determined. These quantities can be directly compared to the observed values for Galactic dSph galaxies. Figure 1 shows three snapshots of the evolution of a typical satellite. The left panel depicts the satellite immediately after the simulation started, the middle one after the first apogalactic passage and the right one shortly after the third apogalacticon. It has dissolved. However, there still exists a measurable density enhancement, which might be identified as a dSph galaxy.

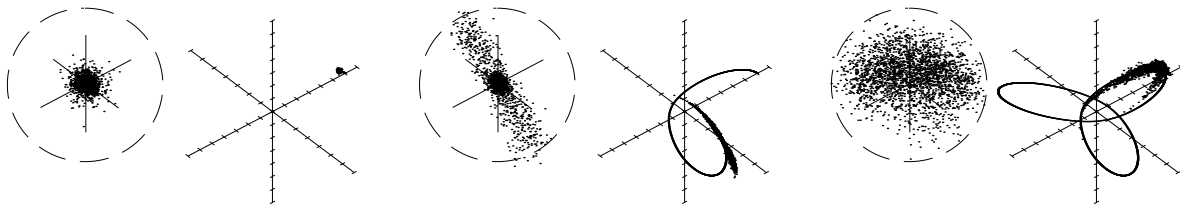


Figure 1: Snapshot of the evolution of a satellite with orbital eccentricity of $e = 0.71$. The right side of each panel plots the distribution of satellite particles at the given time in the Galactic coordinate system. Each of the axes is 140 kpc long. The solid line depicts the trajectory of the density maximum of the satellite until the time of the snapshot. Encircled are enlargements of the central part of the satellite (the total length of each axis is 5 kpc).

The main finding in this studies is that a remnant containing about 1 per cent of the initial satellite mass remains as a long-lived and distinguishable entity after the major disruption event. To an terrestrial observer, this remnant looks strikingly similar to a dSph galaxy. The remnant consists of particles that have phase-space characteristics that reduce spreading along the orbit. Projection effects are also important: an observer who’s line-of-sight sub-

tends a small angle with the orbital path of the satellite sees an apparently brighter remnant with internal sub-clumps and an inflated velocity dispersion. The observer derives values for $(M/L)_{\text{obs}}$ that are much larger than the true mass-to-light ratio $(M/L)_{\text{true}}$ of the particles, because the object is far from virial equilibrium and has a velocity dispersion tensor that is significantly anisotropic. Figure 2 shows in the left panel the evolution of the Lagrange radii of the above satellite and the galactocentric distance of its center-of-mass. The left panel plots the measured central surface brightness μ , the line-of-sight velocity dispersion σ and the derived mass-to-light ratio M/L as function of time.

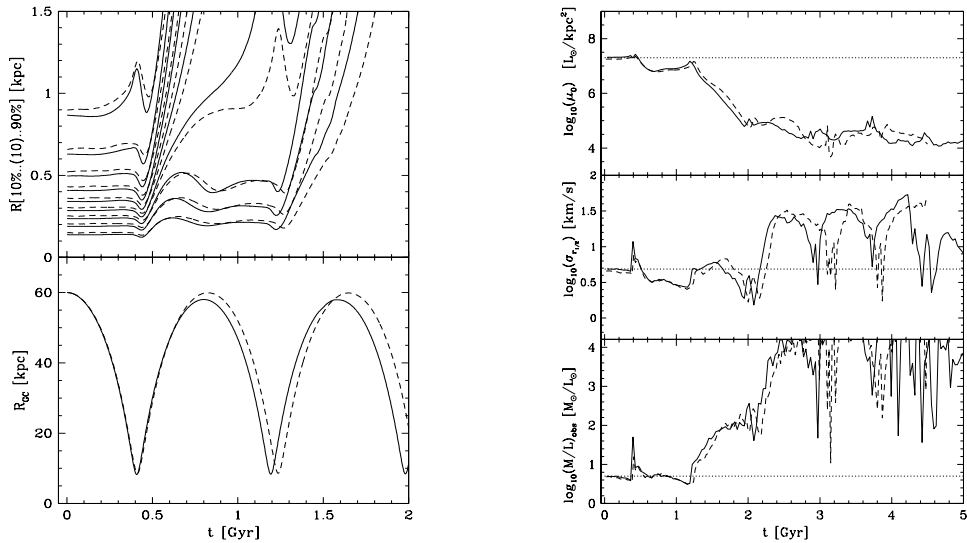


Figure 2: The left side shows the evolution of the radii containing 10, 20, ..., 90 per cent of the total mass of the satellite (top) and the galactocentric distance (bottom) as a function of time. The right side plots the evolution of the central surface brightness μ_0 (top), of the line-of-sight velocity dispersion $\sigma_{1/2}$ within the half-light radius (middle) and of the apparent mass-to-light ratio (bottom). In all panels, the solid line describes the simulation with the nested grid code and the dashed line the one with direct summation on GRAPE.

3 Possible Discriminants

The simulations in K97 and KK98 support the hypothesis that dark matter may not be necessary to account for the structural and kinematical properties of at least some of the Galactic dSph satellites. They furthermore indicate possible diagnostics to discriminate between tidal and dark-matter-dominated models.

3.1 The Preference of Eccentric Orbits

The complete set of simulations discussed in K97 and KK98 shows that there is a well-defined correlation between line-of-sight velocity dispersion and orbital eccentricity. This can be quantified by computing the time average of the observed central line-of-sight velocity dispersion $\langle \sigma_0 \rangle$ over the time interval of 2.5 Gyr after the apparent mass-to-light ratio of

the satellite has exceeded the threshold $(M/L)_{\text{obs}} = 50$. A plot of $\langle\sigma_0\rangle$ as function of the eccentricity is given in figure 3. Satellites initially on eccentric orbits lead to apparently brighter remnants with inflated line-of-sight velocity dispersions, owing to the observer’s line-of-sight being approximately aligned with the orbital path. In this case, particles ahead of and following the remnant add to what the observer may make out to be a dSph galaxy. An observer looking along a very eccentric orbit finds a remnant with a large σ .

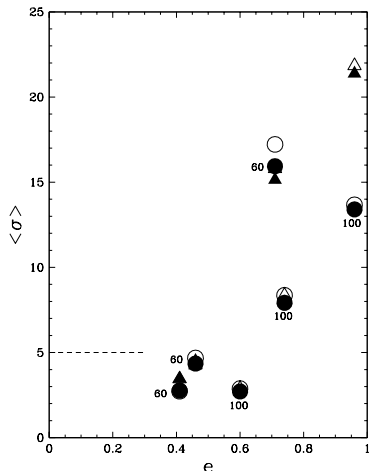


Figure 3: The time-averaged velocity dispersion, computed over the first 2.5 Gyr after $(M/L)_{\text{obs}} \geq 50$ is achieved, as a function of orbital eccentricity e (from KK98). The horizontal dashed line indicates the initial central line-of-sight velocity dispersion.

The velocity dispersions measured in Galactic dSph satellites range from about 6 km/s to 11 km/s (Irwin & Hatzidimitriou 1995, Mateo 1998a). The projection effects imply that, on average, remnants without dark matter and with larger velocity dispersions ought to be on more eccentric orbits and suggests that the Galactic dSph satellites have orbital eccentricities $e > 0.5$. Conversely, a dSph satellite with $e < 0.3$ and $\sigma_0 > 6$ km/s should be dark matter dominated, unless such it has an extreme internal velocity anisotropy with a large velocity dispersion perpendicular to the direction of the orbital path (Kuhn 1993).

3.2 The Width of the Horizontal Branch

A spread of distances leads to a broadening of the giant and horizontal branches in the HR diagram. Sub-clumping along the line-of sight will lead to distinct populations that are separated vertically in the HR diagram. These are important possible observational discriminants, and the horizontal branch is especially well suited for this type of investigation because it is horizontal and blue enough to be less affected by contamination by foreground Galactic field stars. The upper panels in figure 4 show the apparent magnitude distribution of the particles at three different positions across the face of a remnant. The lower panels sample all particles within 1.2 kpc of the density maximum. In the left plot, the angle between the line-of-sight and the orbital trajectory is very small. The radial extent of the remnant is very large and there is considerable scatter in the diagram. On the right side, the remnant is seen almost perpendicular to its orbital motion and its radial depth is very small. Its HR diagram would appear very narrow.

The tidal model therefore predicts considerable scatter in the CMDs of at least some dSph galaxies. For preferentially eccentric orbits, projection effects enhance the extent of the observed remnant along the line-of-sight. This translates into a distribution of stellar magnitudes and subsequently a scatter in the CMD. This feature is observed in some of the

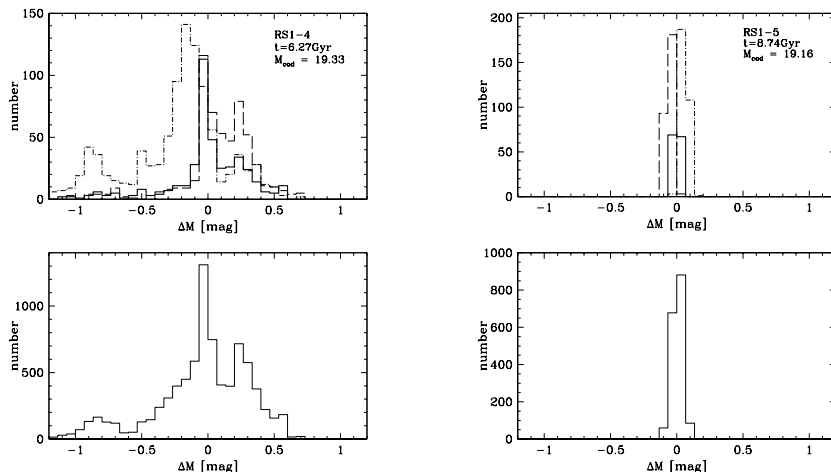


Figure 4: Upper panels: distribution of distance moduli relative to the distance modulus of the remnant’s density maximum at three different positions across the face of the remnant. Lower panel: distribution for all particles appearing projected within a radial distance of 1.2 kpc from the position on the sky of the remnant’s density maximum.

Galactic dSph galaxies (see Grebel 1997 and Da Costa 1997) and is usually interpreted as being a sign of complex star formation histories or metallicity variations. The above model suggests an additional possibility. Probably all three contribute and it seems very difficult to disentangle these effects.

References

- Burkert, A., 1997, ApJ, 474, L99
- Da Costa, G.S., 1997, in “Stellar Astrophysics for the Local Group: A First Step to the Universe”, eds. A. Aparicio & A. Herrero, Cambridge University Press, in press
- Ebisuzaki, T., Makino, J., Fukushige, T., Taiji, M., Sugimoto, D., Ito, T., Okumura, S., 1993, PASJ, 45, 269
- Ferguson, H.C., Binggeli, B., 1994, A&AR, 6, 67
- Grebel, E.K., 1997, Reviews in Modern Astronomy, 10, 29
- Grillmair, C.J., 1998, in the proceeding to the 1997 Santa Cruz Halo Workshop, ed. D. Zaritsky, in press (also astro-ph/9711223)
- Irwin, M., Hatzidimitriou, D., 1995, MNRAS, 277, 1354
- Johnston, K.V., 1997, ApJ submitted (also astro-ph/9710007)
- Johnston, K.V., Spergel, D.N., Hernquist, L., 1995, ApJ, 451, 598
- Klessen, R.S., Kroupa, P., ApJ, 498, in press (also astro-ph/9711350)
- Kroupa, P., 1997, New Astronomy, 2, 139 (K97)
- Kuhn, J.R., 1993, ApJ, 409, L13
- Kuhn, J.R., Smith, H.A., Hawley, S.L., 1996, ApJ, 469, L93
- Mateo, M., 1998a, in: “The Nature of Elliptical Galaxies”, eds. M. Arnaboldi, G.S. Da Costa, & P. Saha, PASP, Vol. 116 (also: astro-ph/9701158)
- Mateo, M., 1998b, ARAA, in press
- Oh, K.S., Lin, D.N.C., Aarseth, S.J., 1995, ApJ, 442, 142
- Olszewski, E.W., 1998, in the proceeding to the 1997 Santa Cruz Halo Workshop, ed. D. Zaritsky, in press (also astro-ph/9712280)
- Piatek, S., Pryor, C., 1995, AJ, 109, 1071

- Pryor, C., 1994, in “Dwarf Galaxies”, eds. G. Meylan & P. Prugniel, ESO Conference and Workshop Proceedings No. 49, ESO, p. 323
- Smith, H.A., Kuhn, J.R., Hawley, S.L., 1998, in “Proper Motions and Galactic Astronomy”, ed. R.M. Humphreys, PASP, in press
- Sugimoto, D., Chikada, Y., Makino, J., Ito, T., Ebisuzaki, T., Umemura, M., 1990, *Nature*, 345, 33
- Tsujimoto, T., Yoshii, Y., Nomoto, K., Matteucci, F., Thielemann, F.-K. & Hashimoto, M., 1997, *ApJ*, 483, 228